1-1-2010

Internal magnetic structure of magnetite nanoparticles at low temperature

Kathryn L. Krycka

Julie A. Borchers

R. A. Booth

C. R. Hogg

Yumi Ijiri
Oberlin College, Yumi.Ijiri@oberlin.edu

See next page for additional authors

Internal magnetic structure of magnetite nanoparticles at low temperature

K. L. Krycka,[1,a)] J. A. Borchers,[1] R. A. Booth,[2] C. R. Hogg,[2] Y. Ijiri,[3] W. C. Chen,[1,4] S. M. Watson,[1] M. Laver,[5] T. R. Gentile,[1] S. Harris,[3] L. R. Dedon,[3] J. J. Rhyne,[6] and S. A. Majetich[2]

[1]*NIST Center for Neutron Research, Gaithersburg, Maryland 20899, USA*
[2]*Carnegie Mellon University, Pittsburgh, Pennsylvania 15213, USA*
[3]*Oberlin College, Oberlin, Ohio 44074, USA*
[4]*Department of Materials Science and Engineering, University of Maryland, College Park, Maryland 20742-2115, USA*
[5]*Paul Scherrer Institut, 5232 Villigen, Switzerland*
[6]*Lujan Neutron Scattering Center, Los Alamos, New Mexico 87545, USA*

(Presented 20 January 2010; received 11 November 2009; accepted 24 November 2009; published online 14 May 2010)

Small-angle neutron scattering with polarization analysis reveals that Fe_3O_4 nanoparticles with 90 Å diameters have ferrimagnetic moments significantly reduced from that of bulk Fe_3O_4 at 10 K, nominal saturation. Combined with previous results for an equivalent applied field at 200 K, a core-disordered shell picture of a spatially reduced ferrimagnetic core emerges, even well below the bulk blocking temperature. Zero-field cooling suggests that this magnetic morphology may be intrinsic to the nanoparticle, rather than field induced, at 10 K. © *2010 American Institute of Physics*. [doi:10.1063/1.3358049]

I. INTRODUCTION

Magnetic nanoparticles are highly desirable for applications including magnetic media, hyperthermia treatment of cancer, and magnetically directed drug delivery. While the optimal level of magnetic coupling or "cross-talk" between nanoparticles can vary dramatically, common to all these applications is a need to predict and either control or work within the framework of these magnetic interactions. However, magnetic coupling is dependent not only on the physical separation and three-dimensional packing arrangement of the nanoparticles but also on their internal magnetic structures of which less in known. Magnetically distinctive shells, for example, have been shown to significantly impact both coupling strength[1] and stability.[2]

Magnetite (Fe_3O_4), a ferrimagnet of moment comparable to that of nickel, is both resistant to oxidation and biocompatible when synthesized under appropriate conditions. Our sample consists of highly monodisperse, 90 Å diameter Fe_3O_4 nanospheres, prepared similar to Ref. 3, with emphasis on monodispersity over biocompatibility. Slowly precipitated from solution, the nanoparticles self assemble into face-centered cubic crystallites[4] with order of up to 1 μm. Reduction in their magnetic moments compared to bulk Fe_3O_4 has led to hypotheses of a disordered, magnetically inactive shell.[5–8] Recently, however, an ordered magnetic shell 10 Å ± 2 Å thick, canted at 90° to the ferrimagnetic core, was detected in an applied field of 1.2 T at 200 K.[9] The aim of this work is to determine if this internal magnetic arrangement changes as the temperature drops below the blocking temperature of 65 K, as determined by magnetometry.

Polarization analyzed small-angle neutron scattering (SANS) is an ideal technique because it can detect the distribution and orientation of magnetic structures with subnanometer resolution. Depending on the direction of the sample moment relative to the neutron spin, a scattering neutron may either undergo spin inversion [spin flip (SF) +− and −+)] or remain in its original orientation [non-spin-flip (NSF) ++ and −−]. Measurement of all four possible cross sections (++,+−,−+,−−) enables full separation of the scattering originating from nuclear structure (N^2), the magnetic structure of moments parallel with an applied field ($M^2_X = M^2_{PARL}$), and the magnetic structure of moments oriented in the two remaining perpendicular directions ($M^2_Y + M^2_Z = M^2_{PERP}$, assuming $M^2_Y = M^2_Z$).[10,11] The observed scattering intensity, I, a function of scattering wave vector, Q, is proportional to the squared absolute value of these spatial Fourier transforms defined as

$$N, M_J(Q) = \sum_K \rho_{K,J} e^{i\vec{Q}\cdot\vec{R}_K}, \quad (1)$$

where J is any Cartesian coordinate, ρ is the structural or magnetic scattering length density, and $\vec{R}_K$ is the relative position of the K^{th} scatterer.

II. EXPERIMENTAL DETAILS

A SANS experiment with polarization involves application of an external magnetic field that defines the axis about which neutron magnetic moments randomly align parallel or antiparallel (arbitrarily denoted as + or −). Polarization is accomplished with an FeSi supermirror cavity, followed by an electromagnetic precession coil employed to reverse orientation at will. Neutron spin analysis of the divergent beam after interaction with the sample is made possible by a ^{3}He spin filter.[12,13] The four scattering cross sections are collected on a two-dimensional (2D) position sensitive detector. After

[a)]Electronic mail: kathryn.krycka@nist.gov.

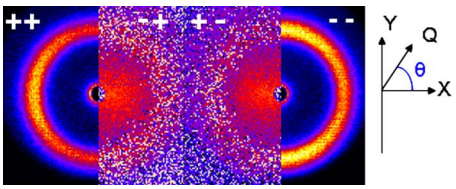

FIG. 1. (Color online) The four cross sections for Fe_3O_4 nanoparticle scattering at 10 K, 0.15 T after correcting for the efficiencies of the polarizing elements. NSF scattering (++,−−) is dominated by N^2 and the interference term, NM_{PARL}. SF scattering (+−,−+) contains only magnetic scattering information.

correcting for the efficiencies of the supermirror, flipper, and ^{3}He analyzer, data taken under zero-field cooled conditions at 10 K in a 0.15 T field are shown in Fig. 1.

To most easily interpret these images, we note that spin-scattering selection rules[9,10] simplify at several key orientations in SANS geometry. With the incoming beam along Z, the applied field along X, and the detector set within the X-Y plane, we have

$$I^{++,--}_{\theta=0^\circ} = N^2 \tag{2}$$

$$I^{++,--}_{\theta=90^\circ} = N^2 + M^2_{PARL} \pm 2NM_{PARL}, \tag{3}$$

$$I^{+-,-+}_{\theta=0^\circ} = M^2_Y + M^2_Z = 2M^2_{PERP}, \tag{4}$$

$$I^{+-,-+}_{\theta=90^\circ} = M^2_Z = M^2_{PERP}, \tag{5}$$

where θ is the angle between the X axis and the projection of Q onto the X-Y plane.

Sector slices of $\pm 10^\circ$ about $\theta=0^\circ$, 90°, taken from the 2D data of Fig. 1, embody the features contained within Eqs. 2–5. Figure 2(a) clearly depicts the +/− interference term of NM_{PARL} in $I^{++,--}$ along the vertical ($\theta=90^\circ$) axis, compared to only N^2 in $I^{++,--}$ along the horizontal ($\theta=0^\circ$) axis. Figure 2(b) shows a twofold increase in $I^{+-,-+}$ along the horizontal ($\theta=0^\circ$) compared to $I^{+-,-+}$ along the vertical ($\theta=90^\circ$), which

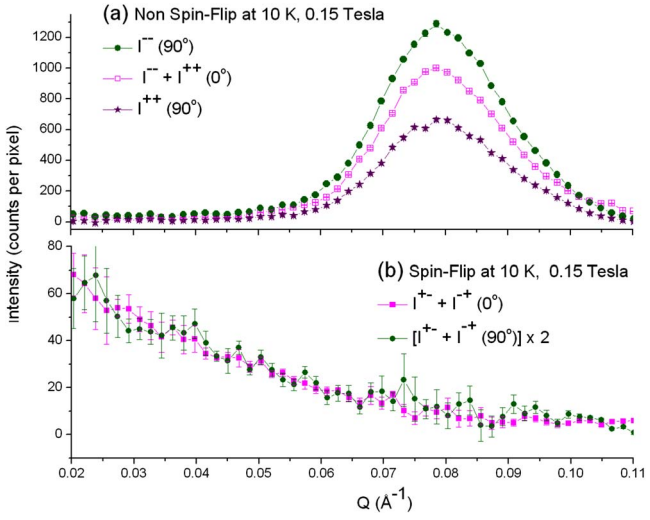

FIG. 2. (Color online) Sector slices of the 2D data. (a) Note the magnitude of NM_{PARL} in comparison with N^2 as both N and M_{PARL} originate from similar structure factors. (b) The 2:1 M^2_{PERP} scattering along $\theta=0^\circ$ and 90°, respectively, indicates that the magnetic structure along the two directions perpendicular to the applied field are equivalent.

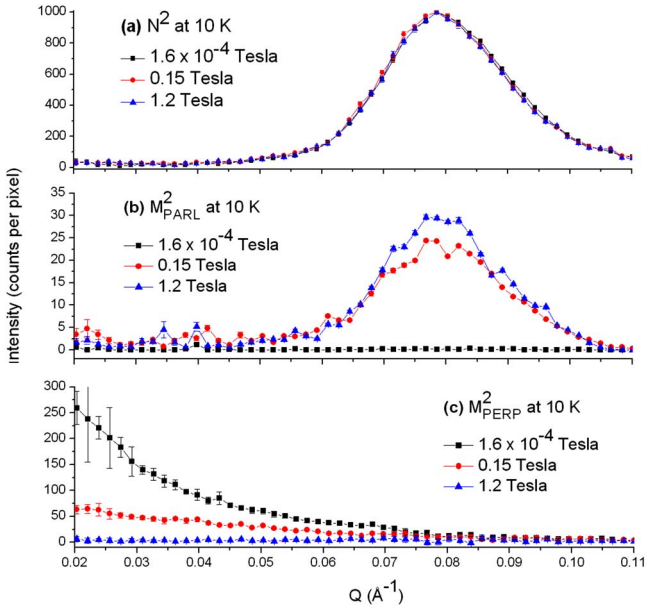

FIG. 3. (Color online) Separation of N^2, M^2_{PARL}, and M^2_{PERP}. (a) N^2 and (b) M^2_{PARL} have similar Bragg peaks at 0.080 $Å^{-1}$ arising from the (111) reflection of the face-centered cubic lattice of nanoparticles. (c) M^2_{PERP} has an increase in low-Q scattering that indicates short-range correlations exist between nanoparticles.

indicates that the magnetic structure along the two directions perpendicular to the applied field are equivalent, as expected.

III. RESULTS

Additional processing of these sector slices allows for the complete separation of N^2, M^2_{PARL}, and M^2_{PERP}.[11] Specifically, we use

$$N^2 = \frac{(I^{++}_{\theta=0^\circ} + I^{--}_{\theta=0^\circ})}{2}, \tag{6}$$

$$M^2_{PARL} = \frac{(I^{--}_{\theta=90^\circ} - I^{++}_{\theta=90^\circ})^2}{16N^2}, \tag{7}$$

$$M^2_{PERP} = \frac{(I^{+-}_{\theta=0^\circ} + I^{-+}_{\theta=0^\circ} + I^{+-}_{\theta=90^\circ} + I^{-+}_{\theta=90^\circ})}{6}. \tag{8}$$

N^2 (Fig. 3(a)) does not change as a function of field and, as such, it is used as a standard by which to normalize the data under different field condition. Its Bragg peak at 0.08 $Å^{-1}$ arises primarily from the (111) face-centered cubic reflection of the nanoparticle lattice of length 136 Å. In comparing M^2_{PARL} and M^2_{PERP} (Fig. 3(a) and 3(b), respectively), it is clear that as the applied field is decreased, the net magnetism along the field direction decreases while simultaneously reappearing as an increase in the moments perpendicular to the applied field. The reason M^2_{PARL} adopts a Bragg peak similar to N^2 is that long-range magnetic ordering, with periodicity of the parent nanoparticle array, is induced when all the nanoparticle moments are forced to align by application of a strong applied field. The nanoparticle lattice structure, however, is not imposed on M^2_{PERP} (and these magnetic correlations peak at a lower-Q value, consistent with shorter-range magnetic correlations).

The Bragg peak ratio of $M^2_{PARL}:N^2$ (Fig. 3(a) and 3(b)) provides a means by which to measure the net magnetic moment of each nanoparticle, independent of the sample volume or mass. For this analysis we assume the structural ρ does not vary from the bulk value for Fe_3O_4 of 6.97×10^{-6} Å^{-2},[14] while the magnetic ρ can deviate somewhat from its bulk value of 1.46×10^{-6} Å^{-2}, corresponding to a magnetization of 5.13×10^5 A/m. If the ferrimagnetic cores occupy exactly the same region as their host nanoparticles, then bulk values would produce a $M^2_{PARL}:N^2$ intensity ratio 0.044. Experimentally, we find this ratio to be 0.032, 0.025, and 0.0027 ± 0.001 at 10 K and fields of 1.2, 0.15, and 0.016 T, respectively. This means that even at conditions of nominal saturation the ferrimagnetic nanoparticle moment is significantly reduced from bulk.

This reduced ferrimagnetic moment could be explained by either a uniform reduction in moment across the entire nanoparticle or by a ferrimagnetic core reduced in spatial extent. In comparison, at 200 K, 1.2 T a $M^2_{PARL}:N^2$ ratio of 0.031 ± 0.001 was measured, while perpendicular magnetic scattering revealed the presence of ordered, canted magnetic shells 10 ± 2Å thick, leading to a core-shell model of magnetism. [9] Given the similarity of the 1.2 T $M^2_{PARL}:N^2$ ratios at 10 K and 200 K, we propose that the two underlying ferrimagnetic structures are in all likelihood equivalent in nominally saturating fields below and above the bulk blocking temperature. The 10 K state, however, differs from the 200 K state in that no scattering evidence for ordered perpendicular magnetic shells was observed.[9] This additionally suggests the probably disordering[5–8] of the magnetic shell upon zero-field cooling to 10 K.

IV. CONCLUSIONS

In summary we have employed SANS with full polarization analysis to measure the ferrimagnetic moment of magnetite nanoparticles below their blocking temperature under a variety of fields. Under nominal saturation, a ferrimagnetic moment significantly reduced from bulk was measured that is consistent with application of the same magnetic field at 200 K. Taken together, this suggests a ferromagnetc core that is reduced in spatial extent within its parent nanoparticle.

Additional experiments, with emphasis on SF scattering from which it is possible to directly access the magnetic moments perpendicular to the applied field, have helped to clarify the role of temperature on magnetic core-shell behavior at high fields. For the future, we are especially keen to determine whether robust magnetic shells exist under reduced field conditions where devices incorporating the nanoparticles will typically be operated, especially at very low temperatures.

ACKNOWLEDGMENTS

This work utilized facilities supported in part by the National Science Foundation under Grant Nos. DMR-0454672, DMR-0704178, and DMR-0804779 and the Department of Energy under Grant No. DE-FG02-08ER40481. Development of the ^{3}He spin filters was supported in part by the Department of Energy. We would like to give special thanks to Andrew Jackson, Cedric Gagnon, and John Barker of the NIST Center for Neutron Research for their efforts in making this experiment successful.

[1] D. Kechrakos, K. N. Trohidou, and M. Vasilakaki, J. Magn. Magn. Mater. **316**, e291 (2007).
[2] J. Nogués, V. Skumryev, J. Sort, S. Stoyanov, and D. Givord, Phys. Rev. Lett. **97**, 157203 (2006).
[3] S. Sun, H. Zeng, D. B. Robinson, S. Raoux, P. M. Rice, S. X. Wang, and G. Li, J. Am. Chem. Soc. **126**, 273 (2004).
[4] D. A. Farrell, Y. Ijiri, C. V. Kelly, J. A. Borchers, J. J. Rhyne, Y. Ding, and S. A. Majetich, J. Magn. Magn. Mater. **303**, 318 (2006).
[5] S.-H. Lee and Y.-S. Kim, J. Appl. Phys. **105**, 07B510 (2009).
[6] J. Curiale, M. Granada, H. E. Troiani, R. D. Sánchez, A. G. Leyva, P. Levy, and K. Samwer, Appl. Phys. Lett. **95**, 043106 (2009).
[7] A. Kovács, K. Sato, V. K. Lazarov, P. L. Galindo, T. J. Konno, and Y. Hirotsu, Phys. Rev. Lett. **103**, 115703 (2009).
[8] C. Westman, S. Jang, C. Kim, S. He, G. Harmon, N. Miller, B. Graves, N. Poudyal, R. Sabirianov, H. Zeng, M. DeMarco, and J. P. Liu, J. Phys. D: Appl. Phys. **41**, 225003 (2008).
[9] K. L. Krycka, R. A. Booth, C. R. Hogg, Y. Ijiri, J. A. Borchers, W. C. Chen, S. M. Watson, M. Laver, T. R. Gentile, L. R. Dedon, S. Harris, J. J. Rhyne, and S. A. Majetich, "Core-shell magnetic morphology of structurally uniform magnetite nanoparticles," Phys. Rev. Lett. (submitted).
[10] R. M. Moon, T. Riste, and W. C. Koehler, Phys. Rev. **181**, 920 (1969).
[11] K. L. Krycka, R. A. Booth, J. A. Borchers, W. C. Chen, C. Conlon, T. R. Gentile, C. Hogg, Y. Ijiri, M. Laver, B. B. Maranville, S. A. Majetich, J. J. Rhyne, and S. M. Watson, Physica B **404**, 2561 (2009).
[12] T. R. Gentile, G. L. Jones, A. K. Thompson, J. Barker, C. J. Glinka, B. Hammouda, and J. W. Lynn, J. Appl. Crystallogr. **33**, 771 (2000).
[13] W. C. Chen, R. Erwin, J. W. McIver III, S. Watson, C. B. Fu, T. R. Gentile, J. A. Borchers, J. W. Lynn, and G. L. Jones, Physica B **404**, 2663 (2009).
[14] M. R. Fitzsimmons and C. F. Majkrzak, *Modern Techniques for Characterizing Magnetic Materials* (Kluwer Academic, Dordrecht, 2005).